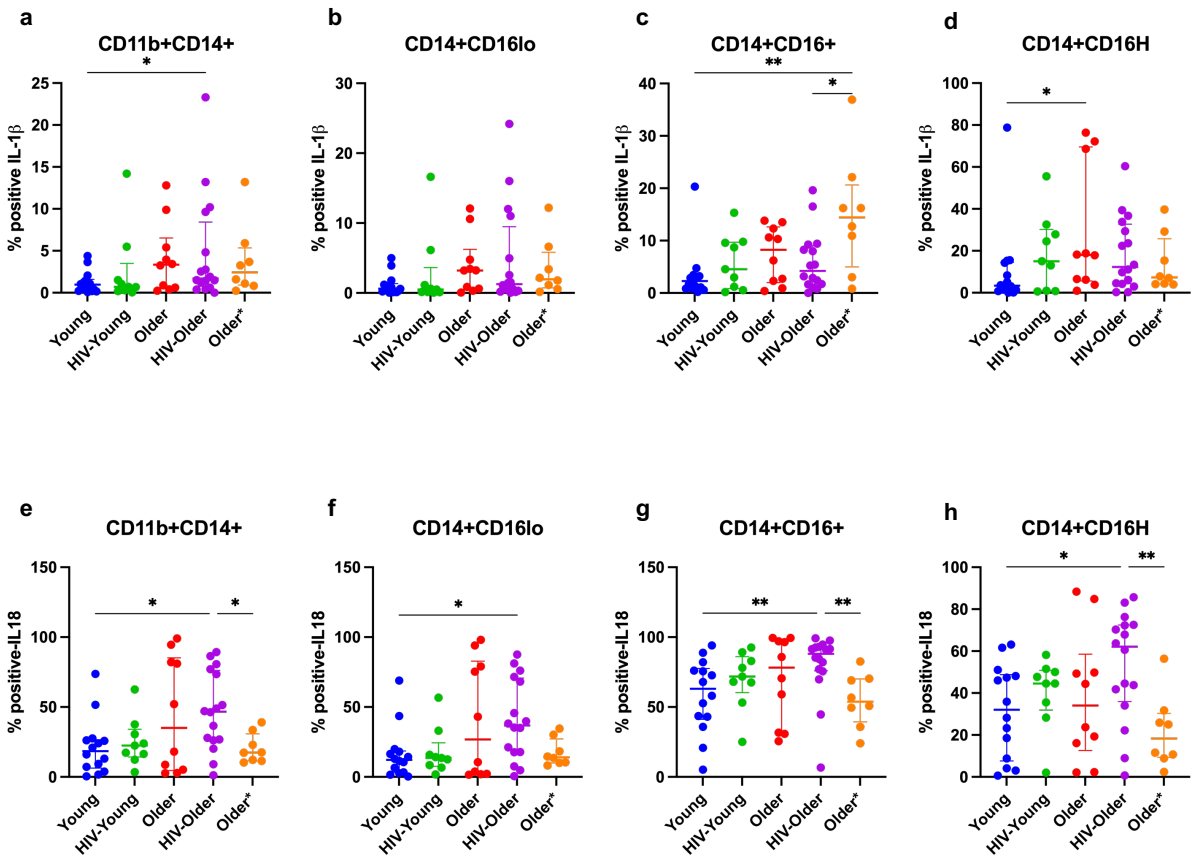
Supplementary Figures

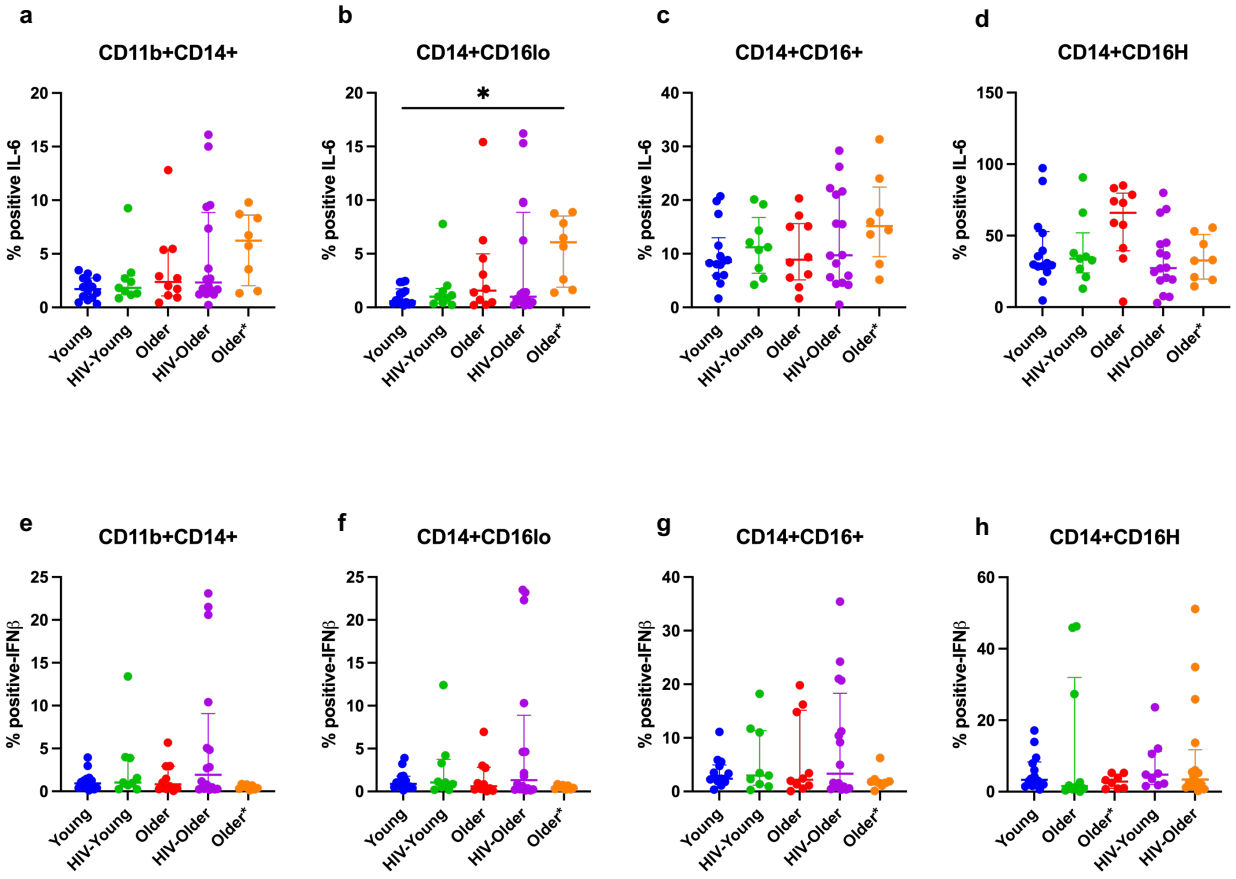
NLRP3 Inflammasome Activation Dynamics are Shaped by Age, HIV-infection and Co-morbid Conditions

Shanshan Du[1]*, Archit Kumar[1]*, Bill Lee[1], Allen Esterly [1], Christopher Radcliffe[1], Lydia Barakat [3], Sui Tsang[2], Allison Nelson[1], Irene Matos[1], Brent Vander Wyk[2], Albert C Shaw[1], and Heidi J Zapata[1]

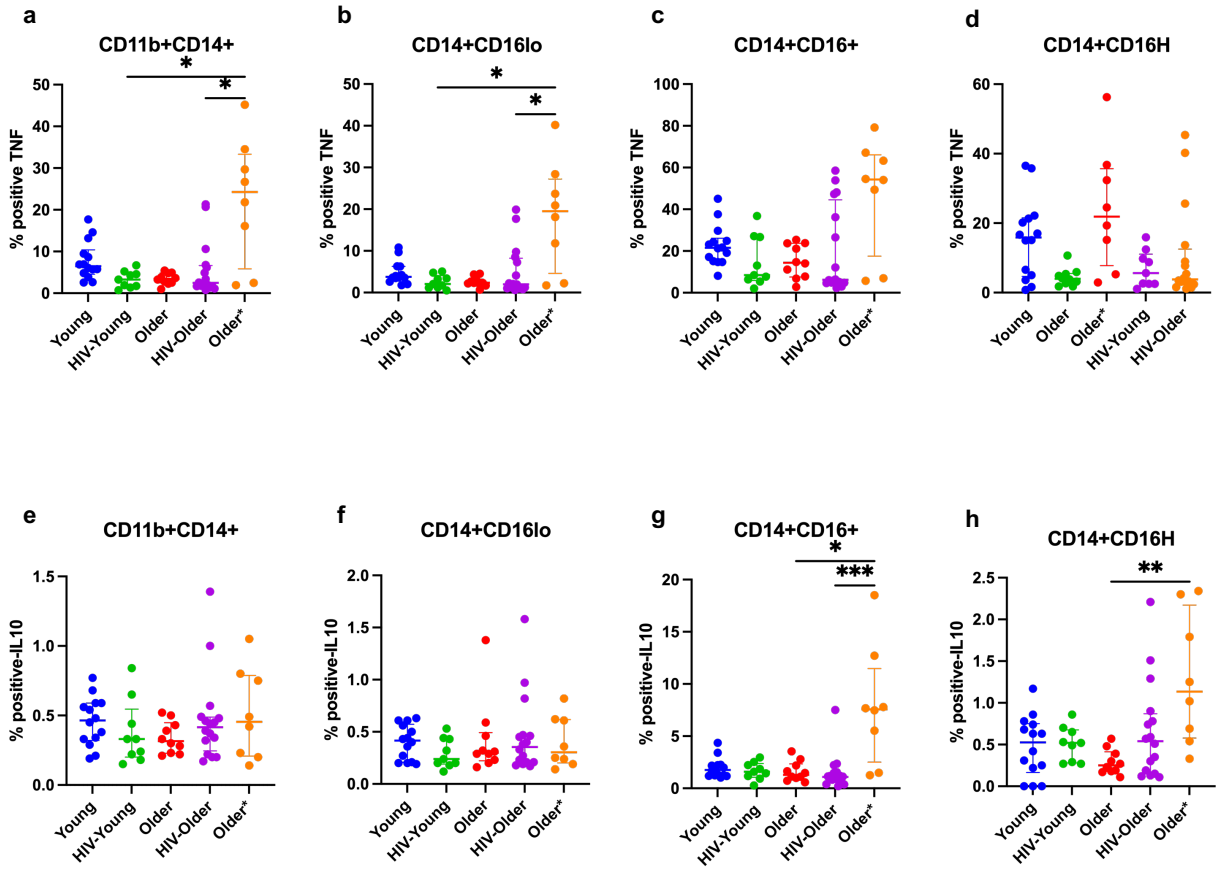
[1] Yale School of Medicine, Section of Infectious Diseases, Department of Internal Medicine, New Haven CT, [2] Yale University Program on Aging, [3] Yale University, Yale AIDS Care Program, New Haven, CT.



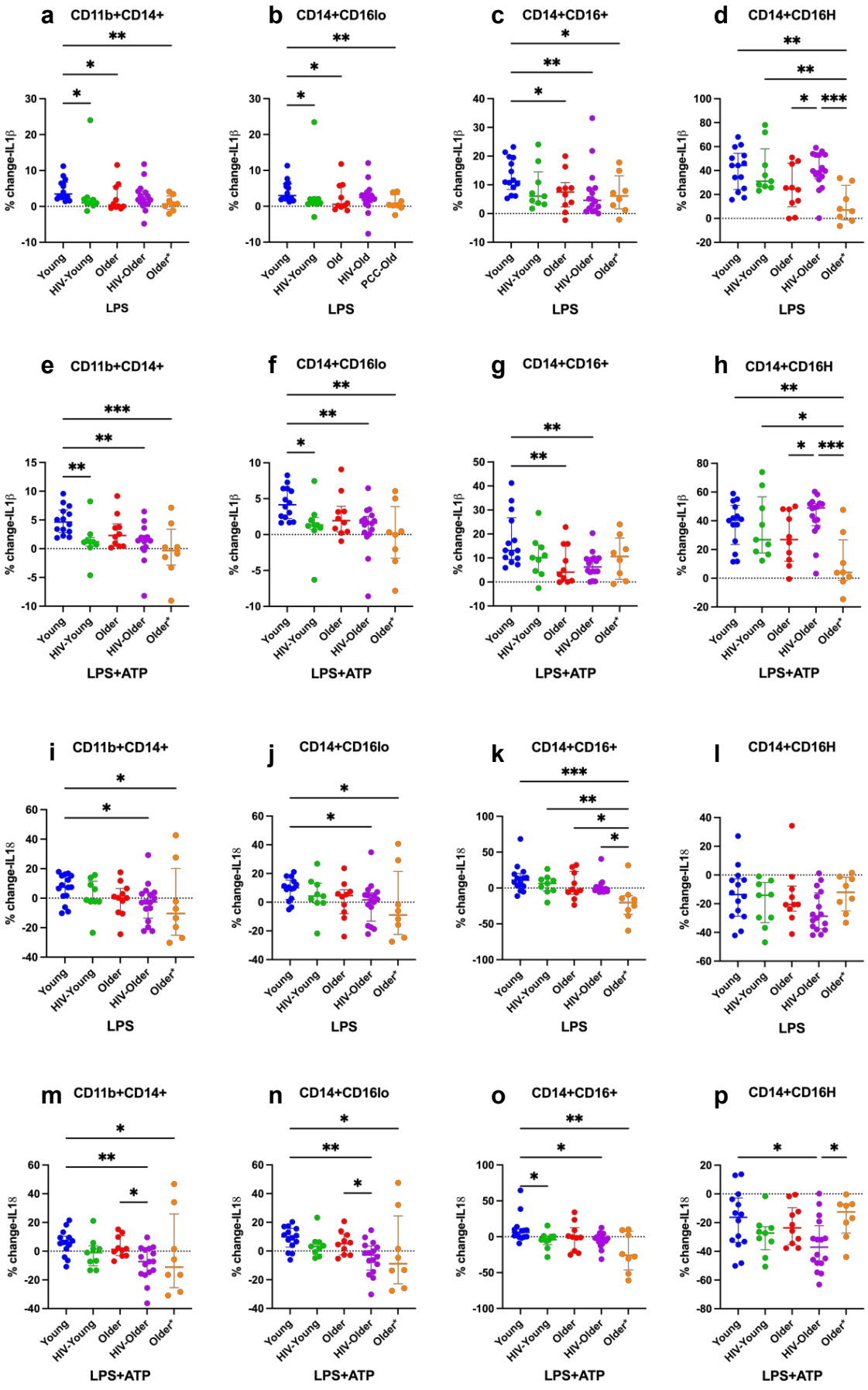
Supplementary Figure 1 | Flow cytometry analysis of IL-1β- and IL-18-positive monocytes across five cohorts at baseline. Each dot represents an individual sample; different colors indicate distinct cohorts. The percentage of cytokine-positive cells is shown for each monocyte subset ($CD11b^{+}CD14^{+}$, $CD14^{+}CD16^{lo}$, $CD14^{+}CD16^{+}$, and $CD14^{+}CD16^{H}$). Statistical significance was assessed using the Kruskal–Wallis test. *$p < 0.05$, **$p < 0.01$. Error Bars represent median ± interquartile range.



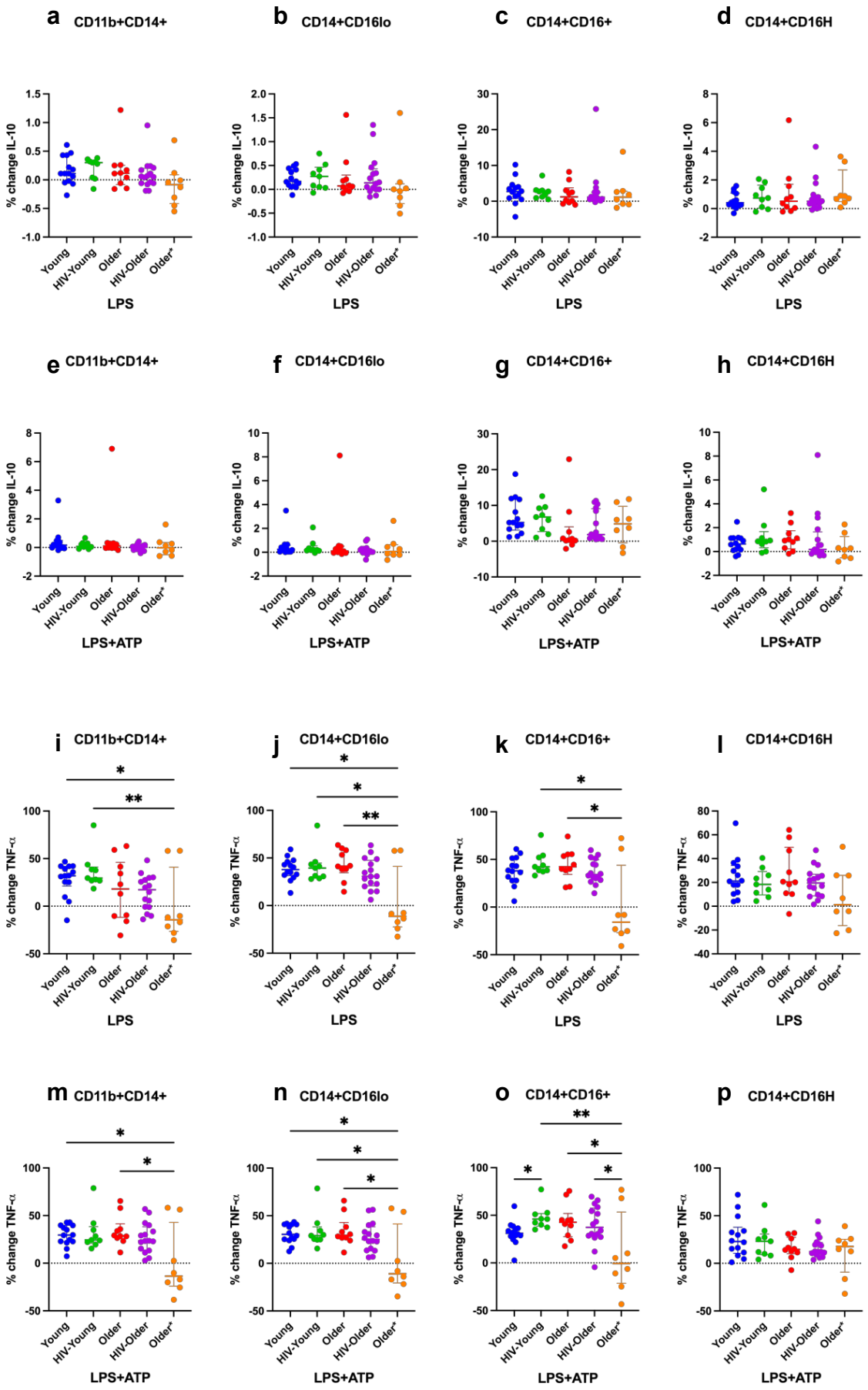
Supplementary Figure 2 | Flow cytometry analysis of IL-6 and IFNβ-positive monocytes across five cohorts at baseline. Each dot represents an individual sample, with different colors corresponding to distinct cohorts. The percentage of cytokine-positive cells is quantified for each monocyte subset ($CD11b^{+}CD14^{+}$, $CD14^{+}CD16^{lo}$, $CD14^{+}CD16^{+}$, $CD14^{+}CD16^{H}$). Statistical significance was assessed using the Kruskal-Wallis test, with asterisks (*$p < 0.05$; ** $p < 0.01$) indicating significant differences between groups. Error bars represent the median with interquartile range.



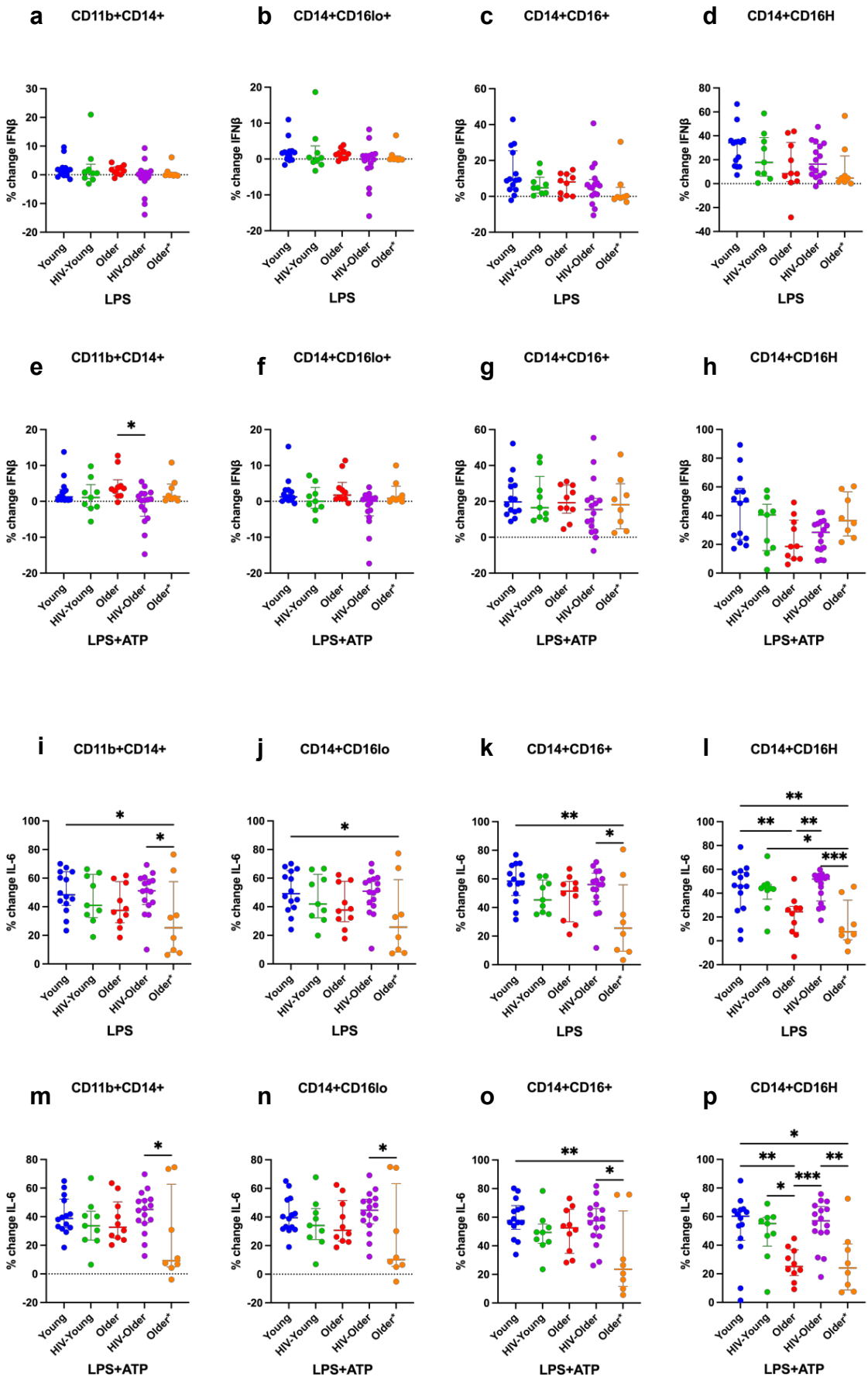
Supplementary Figure 3 | Flow cytometry analysis of TNF-α and IL-10-positive monocytes across five cohorts at baseline. Each dot represents an individual sample, with different colors corresponding to distinct cohorts. The percentage of cytokine-positive cells is quantified for each monocyte subset ($CD11b^{+}CD14^{+}$, $CD14^{+}CD16^{lo}$, $CD14^{+}CD16^{+}$, $CD14^{+}CD16^{H}$). Statistical significance was assessed using the Kruskal-Wallis test, with asterisks (*$p < 0.05$; **$p < 0.01$) indicating significant differences between groups. Error bars represent the median with interquartile range.


a CD11b+CD14+
b CD14+CD16lo
c CD14+CD16+
d CD14+CD16H
e CD11b+CD14+
f CD14+CD16lo
g CD14+CD16+
h CD14+CD16H
i CD11b+CD14+
j CD14+CD16lo
k CD14+CD16+
l CD14+CD16H
m CD11b+CD14+
n CD14+CD16lo
o CD14+CD16+
p CD14+CD16H
% change-IL1β
% change-IL18
Young
HIV-Young
Older
Old
HIV-Old
PCC-Old
HIV-Older
Older*
LPS
LPS+ATP

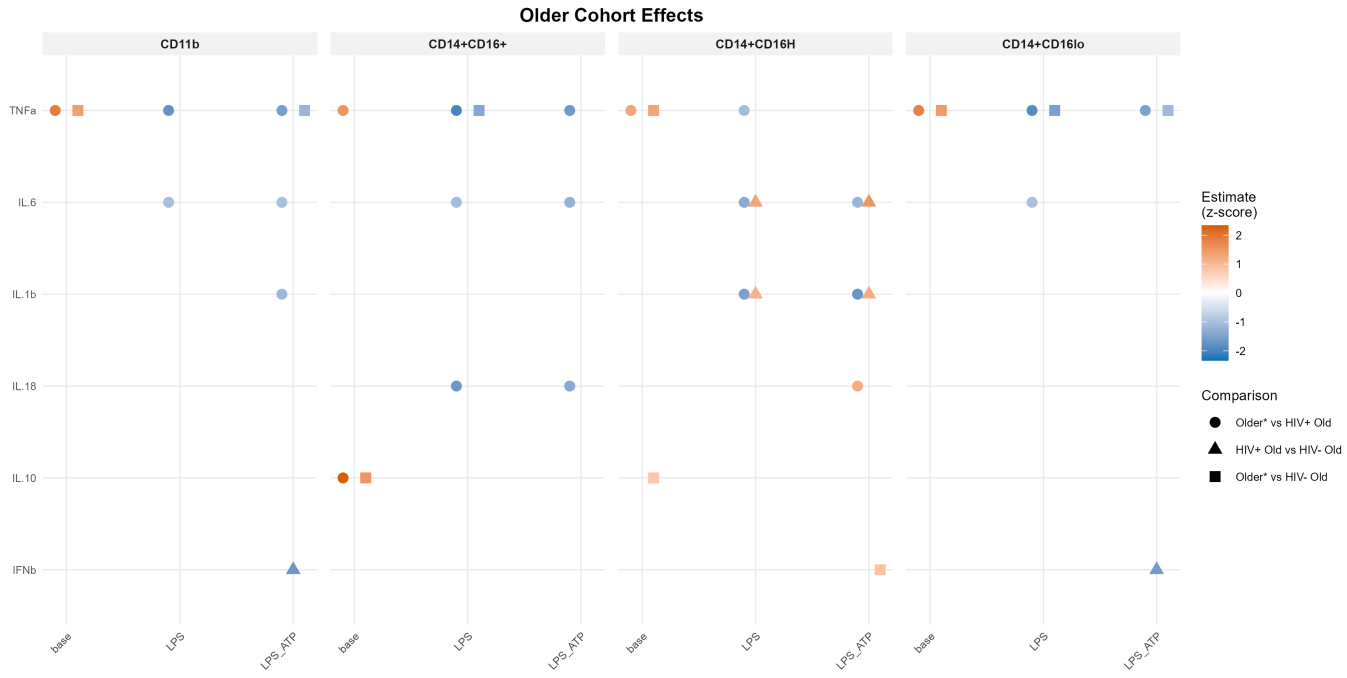
Supplementary Figure 4 | Flow cytometry analysis of IL-1β (a–h) and IL-18 (i–p) expression in monocyte subsets across five cohorts following LPS or LPS + ATP stimulation. Each dot represents an individual sample, with color indicating cohort identity. Cytokine-positive cells were quantified within the following monocyte subsets: $CD11b^{+}CD14^{+}$, $CD14^{+}CD16^{lo}$, $CD14^{+}CD16^{+}$, and $CD14^{+}CD16^{H}$. % change of cytokine with stimulation is shown on y-axis. Statistical comparisons were performed using the Kruskal–Wallis test; *$p < 0.05$, **$p < 0.01$. Error bars indicate median ± interquartile range.


a CD11b+CD14+
b CD14+CD16lo
c CD14+CD16+
d CD14+CD16H
e CD11b+CD14+
f CD14+CD16lo
g CD14+CD16+
h CD14+CD16H
i CD11b+CD14+
j CD14+CD16lo
k CD14+CD16+
l CD14+CD16H
m CD11b+CD14+
n CD14+CD16lo
o CD14+CD16+
p CD14+CD16H
% change IL-10
% change TNF-α
Young
HIV-Young
Older
HIV-Older
Older*
LPS
LPS+ATP

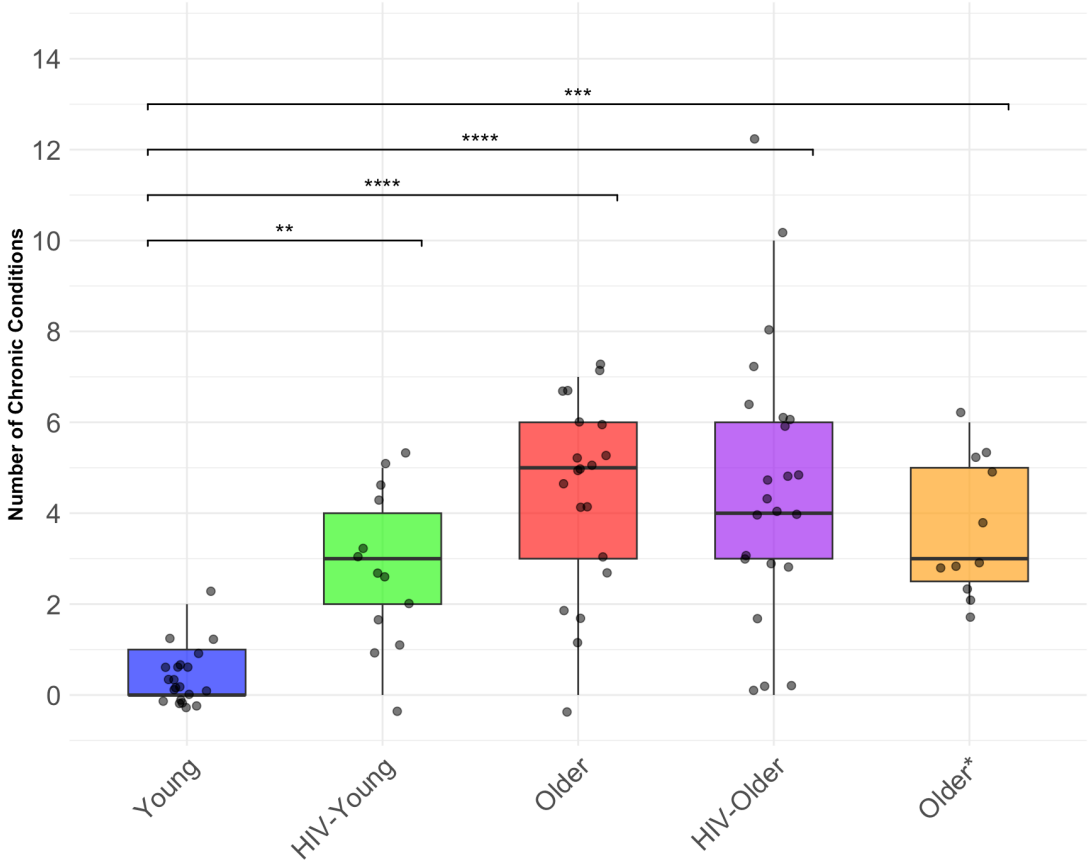
Supplementary Figure 5 | Flow cytometry analysis of IL-10 (a–h) and TNF-α (i–p) expression in monocyte subsets across five cohorts following LPS or LPS + ATP stimulation. Each dot represents an individual sample, with color indicating cohort identity. Cytokine-positive cells were quantified within the following monocyte subsets: $CD11b^{+}CD14^{+}$, $CD14^{+}CD16^{lo}$, $CD14^{+}CD16^{+}$, and $CD14^{+}CD16^{H}$. % change of cytokine with stimulation is shown on y-axis. Statistical comparisons were performed using the Kruskal–Wallis test; *$p < 0.05$, **$p < 0.01$. Error bars indicate median ± interquartile range.


a
CD11b+CD14+
b
CD14+CD16lo+
c
CD14+CD16+
d
CD14+CD16H
% change IFNβ
Young
HIV-Young
Older
HIV-Older
Older*
LPS
e
CD11b+CD14+
f
CD14+CD16lo+
g
CD14+CD16+
h
CD14+CD16H
LPS+ATP
i
CD11b+CD14+
j
CD14+CD16lo
k
CD14+CD16+
l
CD14+CD16H
% change IL-6
m
CD11b+CD14+
n
CD14+CD16lo
o
CD14+CD16+
p
CD14+CD16H

Supplementary Figure 6 | Flow cytometry analysis of IFNβ (a–h) and IL-6 (i–p) expression in monocyte subsets across five cohorts following LPS or LPS + ATP stimulation. Each dot represents one biological replicate, with color indicating cohort identity. Cytokine-positive cells were quantified within the following monocyte subsets: $CD11b^{+}CD14^{+}$, $CD14^{+}CD16^{lo}$, $CD14^{+}CD16^{+}$, and $CD14^{+}CD16^{H}$. % change of cytokine with stimulation is shown on y-axis. Statistical comparisons were performed using the Kruskal–Wallis test; *$p < 0.05$, **$p < 0.01$. Error bars indicate median ± interquartile range.

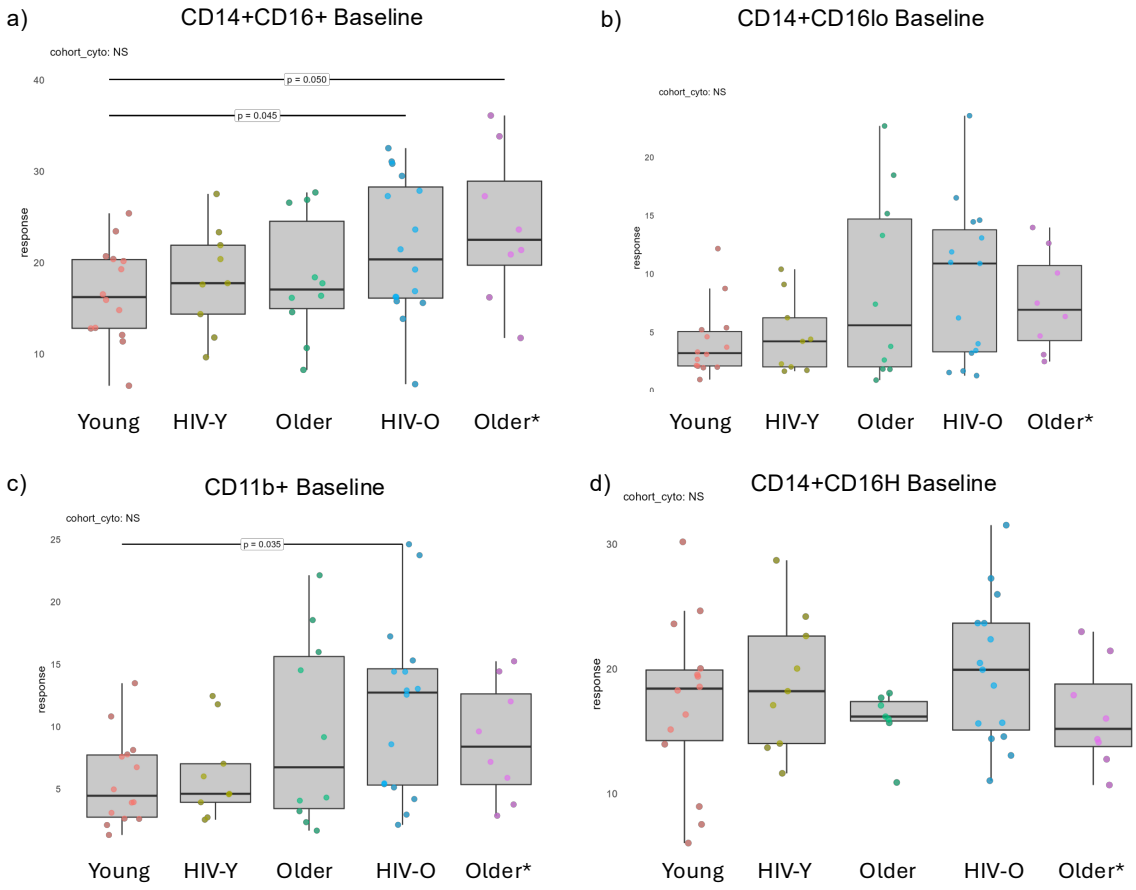


Supplemental Figure 7 | Overview of Older Cohort Effects on Cytokine Production. This figure depicts the direction and magnitude of significant pairwise comparisons between Older* vs HIV-positive Older (circles), HIV-positive Older vs HIV-negative Older (Triangles), and Older* vs HIV-negative Older (squares). Orange indicates upregulation of the first group relative to the second, while blue represents down regulation. Non-significant differences were excluded from the plot. Responses were z-scored within each cell type x marker combination, separately by stimulation class.



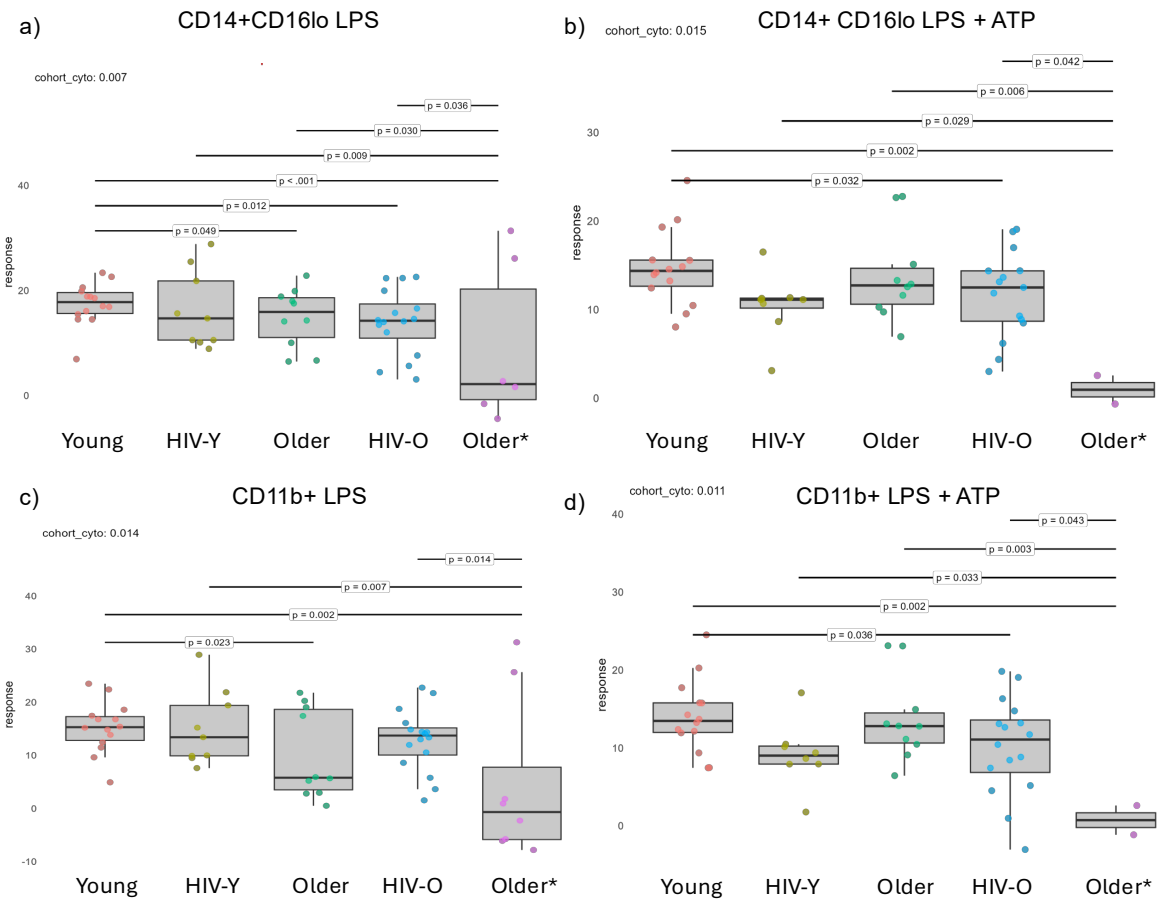
Supplemental Figure 8 | Number of Chronic Conditions Across Cohorts.

Boxplots display the median (center line), interquartile range (box), and 1.5×IQR (whiskers), with individual observations overlaid as jittered points. Pairwise comparisons between Young and all other groups were conducted; significance brackets indicate ** p<0.01, *** p<0.001, **** p<0.0001.

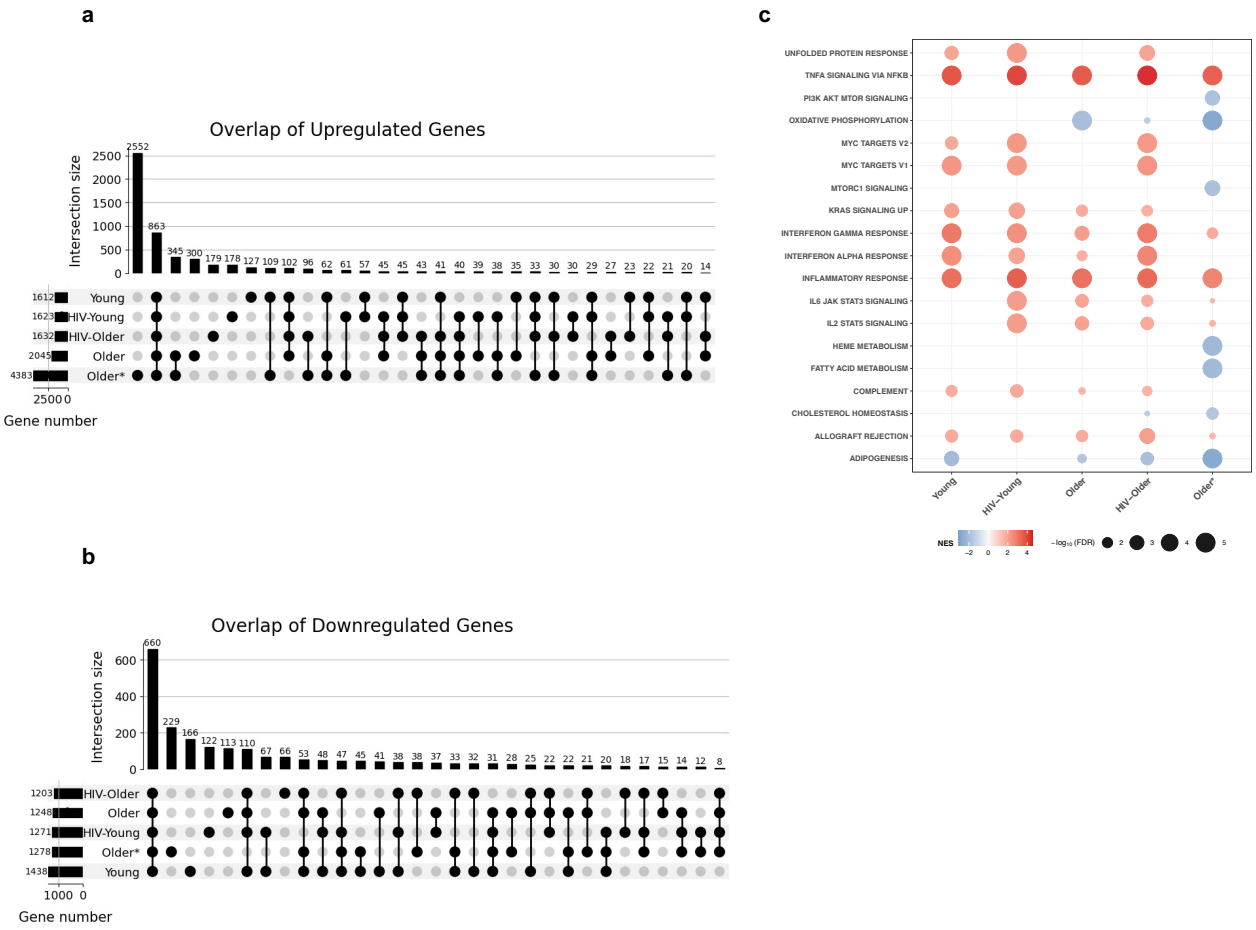


Supplemental Figure 9 | Aggregate Measure of Cytokines at Baseline.

We took an average of all cytokines (aggregate measure) ((TNF-α +IL-1β + IL-18 + IL-6 + IL-10 + IFN-β)/6). Boxplots display the median (center line), interquartile range (box), and 1.5×IQR (whiskers), with individual observations overlaid as colored points (color denotes cohort). Panels show frequencies of **(a)** CD14+CD16+(inflammatory), b) CD14+ CD16lo (classical), c) CD11b+CD14+ (activated monocytes), and d) CD14+ CD16H (non-classical/intermediate) monocytes at baseline. Groups are as defined in Figure 1 (Young, HIV-Y, Older, HIV-O, Older*). A linear model including cohort as a covariate was used for between-group comparisons; the cohort term was non-significant (NS) for all panels. Nominal p-values are shown for pairwise comparisons that reached statistical significance ($p < 0.05$); all other pairwise comparisons were non-significant.



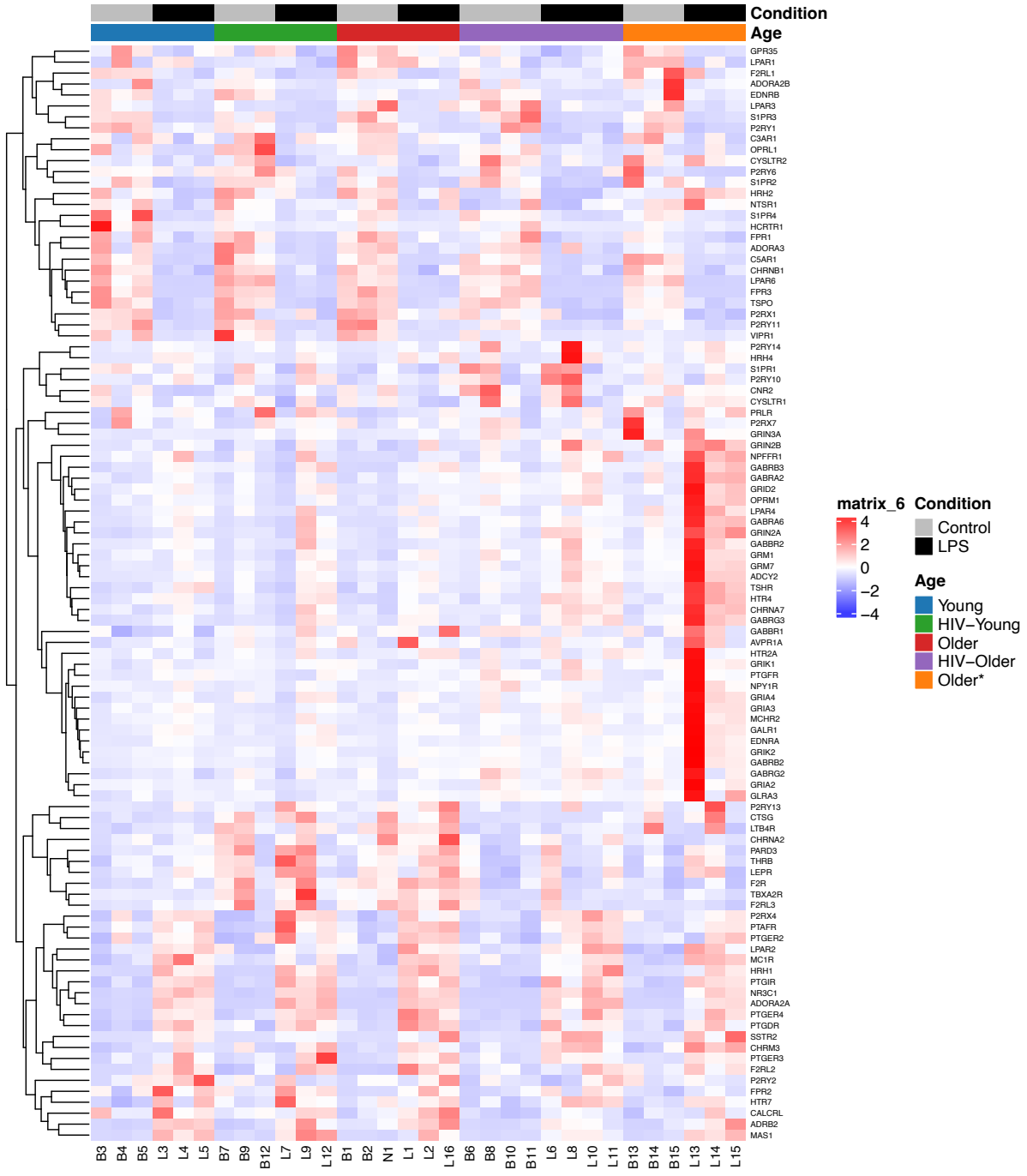
Supplemental Figure 10 | Aggregate Measure of Cytokines with Stimulation. We took an average of all cytokines (aggregate measure) ((TNF-α +IL-1β + IL-18 + IL-6 + IL-10 + IFN-β)/6). Boxplots display the median (center line), interquartile range (box), and 1.5×IQR (whiskers), with individual observations overlaid as colored points (color denotes cohort). Panels show frequencies of (a) CD14+CD16lo monocytes after LPS stimulation, (b) CD14+CD16lo monocytes after LPS+ATP stimulation, (c) CD11b+ monocytes after LPS stimulation, and (d) CD11b+ monocytes after LPS+ATP stimulation. Groups are as defined in Supplemental Figure 9 (Young, HIV-Y, Older, HIV-O, Older*). A linear model including cytometry cohort as a covariate was used for between-group comparisons. Nominal p-values are shown for pairwise comparisons reaching statistical significance ($p < 0.05$); all other pairwise comparisons were non-significant.



Supplementary Figure 11 | Transcriptional responses to LPS stimulation across five cohorts: differentially expressed genes and pathway enrichment analysis.

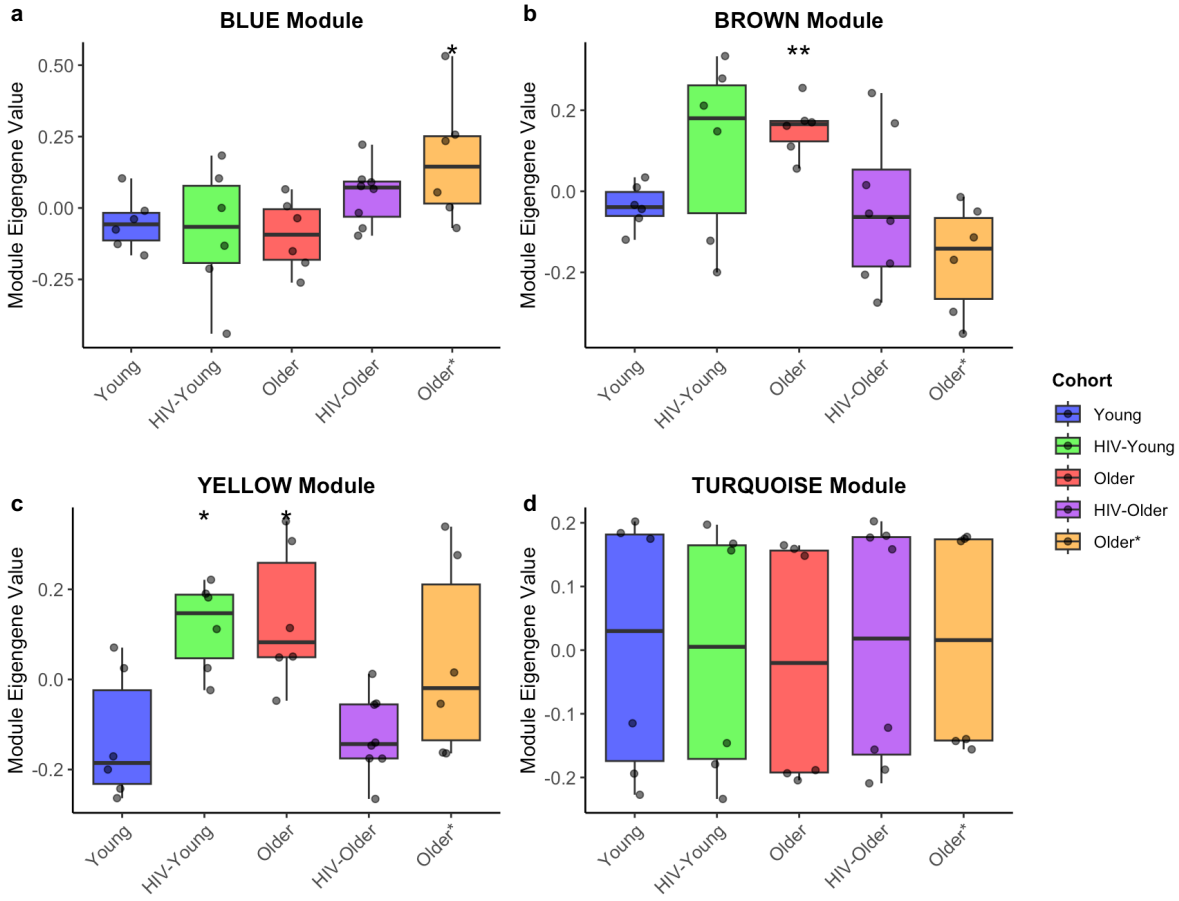
(a) UpSet plot depicting overlap of upregulated genes ($\log_2$ fold-change ≥ 1.2, adj. $p < 0.05$) across five cohorts comparing LPS stimulation to control. Bar heights represent intersection sizes; left horizontal bars indicate the total number of upregulated genes per cohort. Connected dots denote gene sets shared across cohorts. (b) UpSet plot showing overlap of downregulated genes ($\log_2$ fold-change ≤ –1.2, adj. $p < 0.05$) across the same cohorts. Bar heights represent intersection sizes; left horizontal bars indicate the total number of downregulated genes per cohort. Connected dots denote overlapping gene sets. (c) GSEA of LPS-stimulated vs control monocytes within each cohort independently. Dot plot showing significantly enriched Hallmark pathways (FDR < 5%) for each cohort. Node color represents

normalized enrichment score (NES; red: upregulation; blue: downregulation). Node size represents $-\log_{10}$(FDR). Pathways are ordered by mean NES across cohorts. For visualization, FDR values of 0 were adjusted to 0.00001.

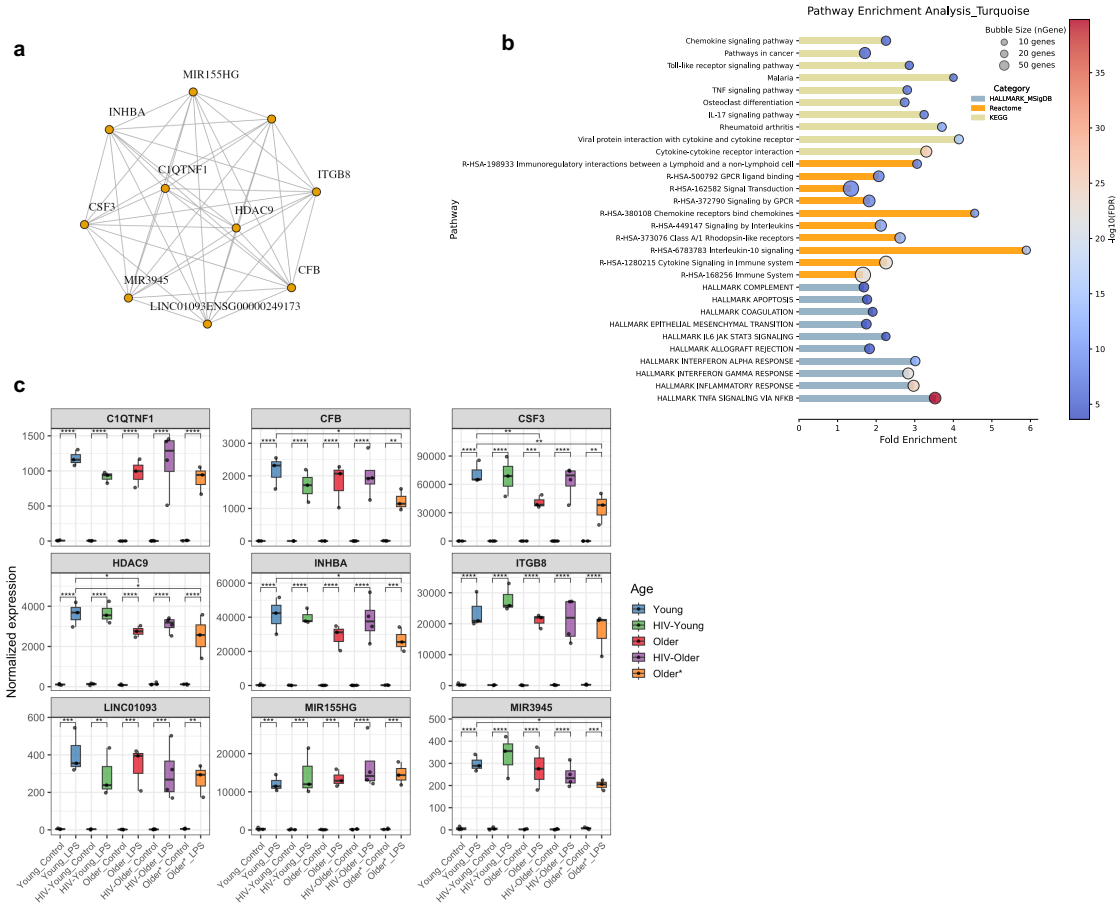


Supplementary Figure 12 | Transcriptomic profile of neuroactive ligand–receptor interaction pathway genes. Heatmap showing the scaled expression (row z-score) of the top 100 most variable genes (by variance across samples) from the KEGG “Neuroactive ligand–receptor interaction” pathway (hsa04080). Each column represents an individual sample, annotated by age group and stimulation condition, and each row corresponds to a

pathway gene. Color scale indicates relative expression, from low (blue) to high (red). Rows are ordered by hierarchical clustering.

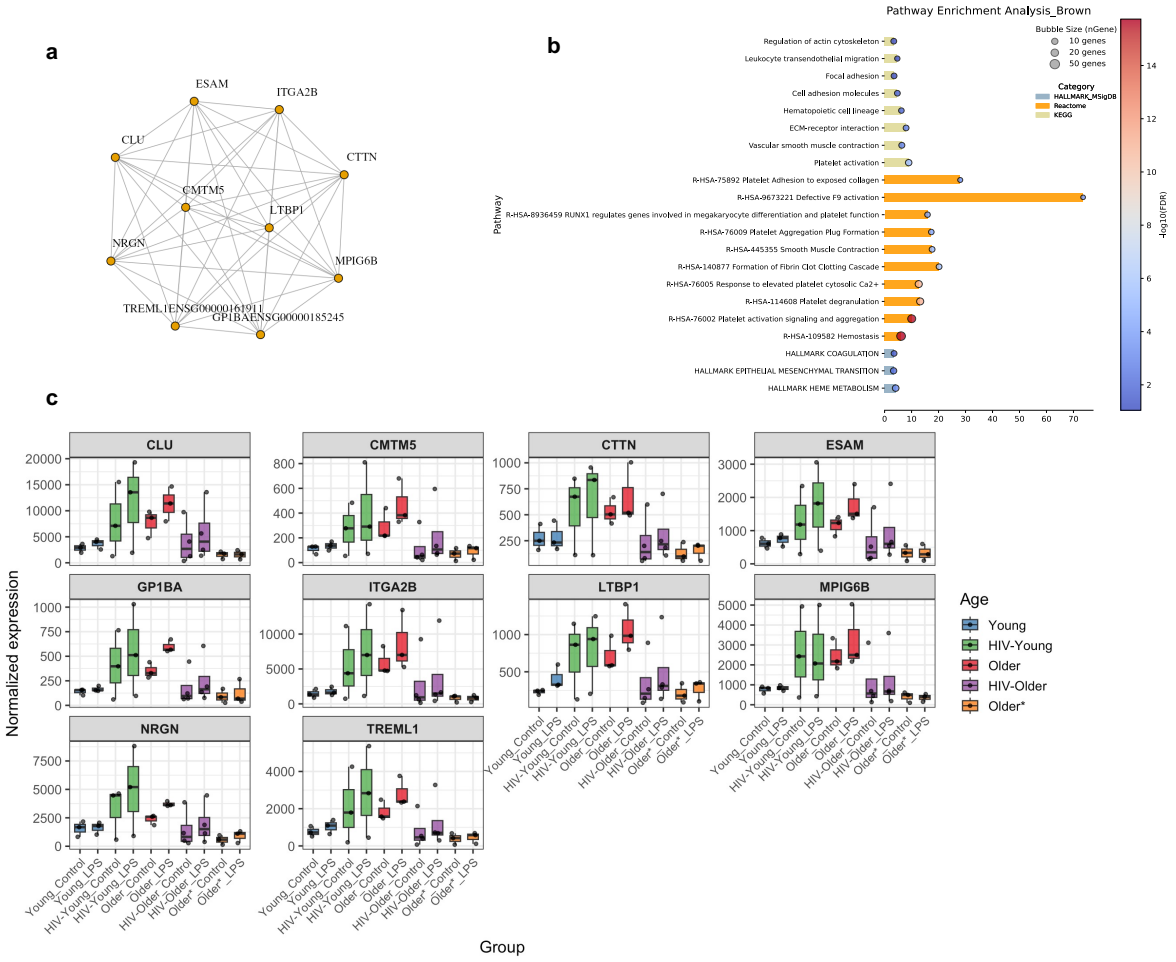


Supplementary Figure 13 | Comparative Analysis of Co-expression Module Activity Across Aging and HIV Infection Cohorts. Four-panel visualization of module eigengene comparisons for the blue module, brown module, yellow module, and turquoise module across five experimental cohorts (box color denotes cohort). Each panel displays box plots of module eigengene values with individual data points overlaid. Statistical comparisons were performed using Wilcoxon rank-sum tests with the Young cohort as the reference group. Significance levels: *$p < 0.05$, **$p < 0.01$, ***$p < 0.001$; non-significant comparisons ($p \geq 0.05$) are not displayed.

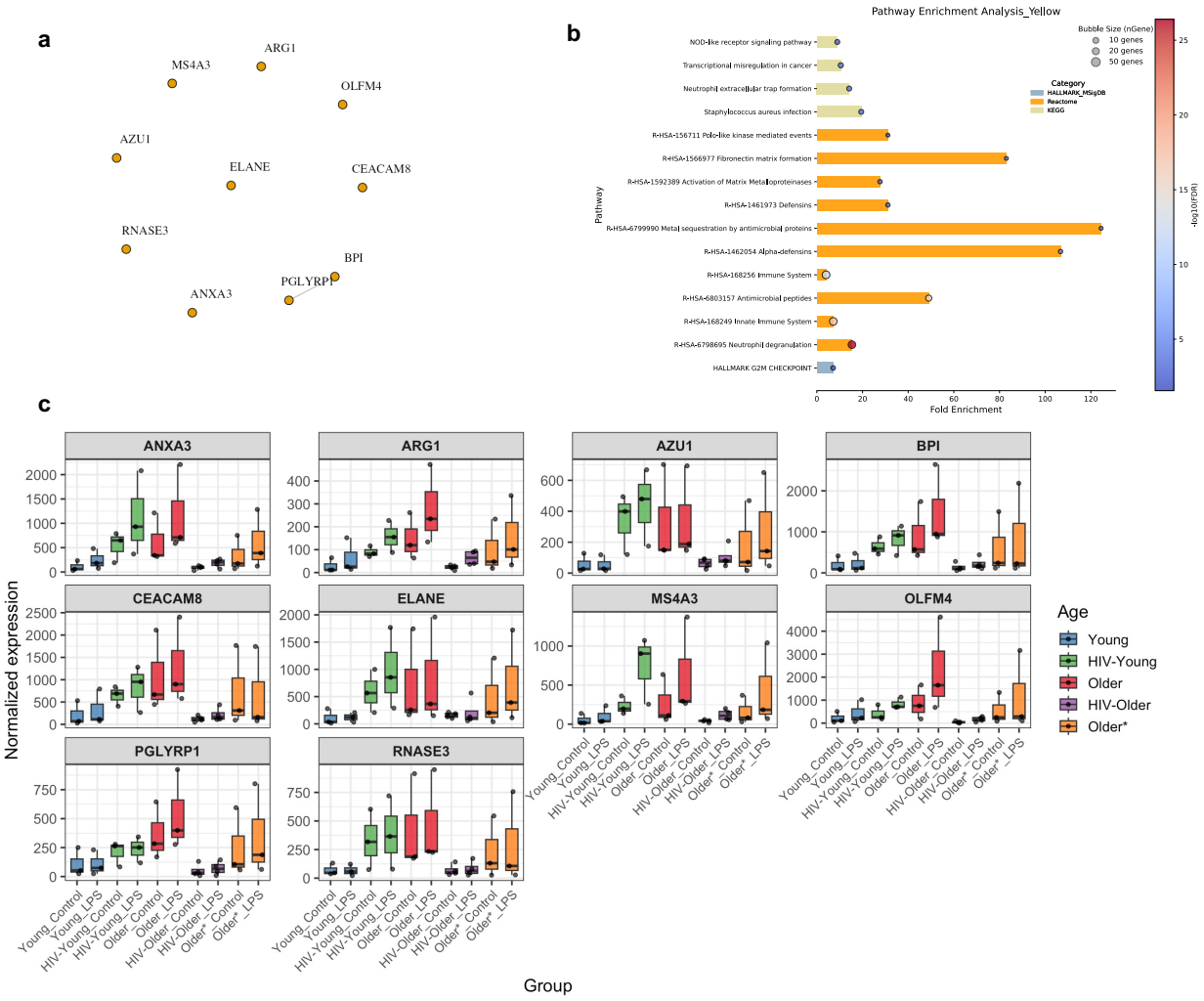


Supplementary Figure 14 |Functional characterization of gene co-expression modules identified by WGCNA module Turquoise. (a) Co-expression network of the turquoise module highlighting hub genes (b) Pathway enrichment analysis for the turquoise module, based on KEGG, Reactome, and MSigDB Hallmark databases. Enriched pathways include cytokine–cytokine receptor interaction, chemokine signaling, Toll-like receptor signaling, and inflammatory response. Bubble size denotes the number of associated genes, while bubble color indicates pathway significance ($-\log_{10}$(FDR)). (c) Boxplot of normalized hub gene expression levels across cohorts and conditions of module turquoise across five cohorts (Young, HIV-Young, Older, HIV-Older, and Older*). Boxplot center lines, medians; bounds,

interquartile range (IQR); whiskers, 1.5× IQR; dots, individual replicates. Colors as indicated. Two-tailed Student's t-tests with Benjamini–Hochberg FDR correction; adjusted p-values (q): *$p < 0.05$, **$p < 0.01$, ***$p < 0.001$. Comparisons: within-cohort (Control vs LPS) and between-cohort at baseline or after LPS (see panel annotations).

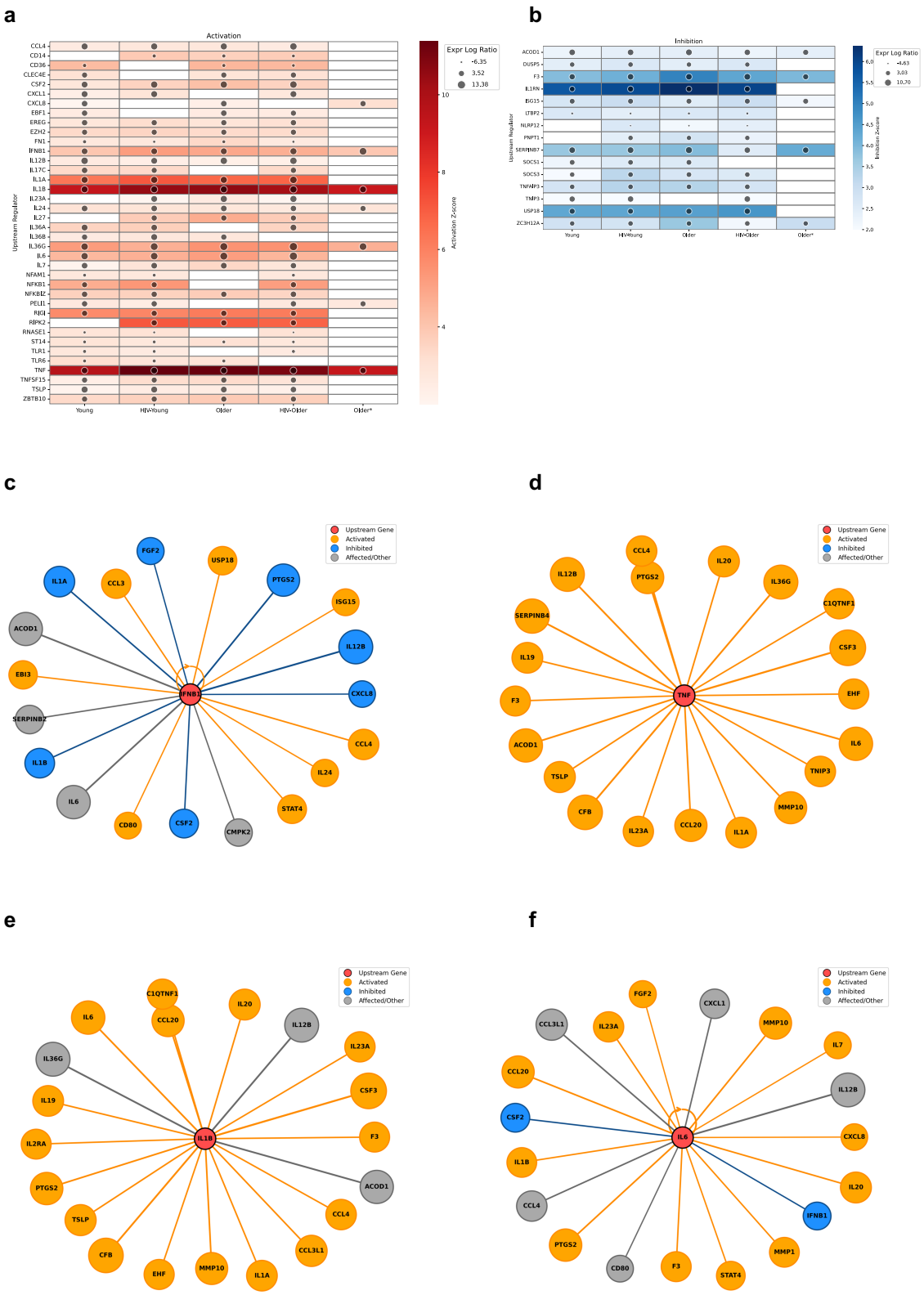


Supplementary Figure 15 | Functional characterization of gene co-expression modules identified by WGCNA module brown. (a) Co-expression network of the brown module highlighting hub genes (b) Enrichment analysis for the brown module reveals pathways related to platelet activation, vascular homeostasis, and hemostasis, including platelet activation, ECM–receptor interaction, and smooth muscle contraction. Bubble size reflects gene count per pathway; color denotes statistical significance ($-\log_{10}$(FDR)). (c) Boxplot of normalized hub gene expression levels across cohorts and conditions of module brown across five cohorts (Young, HIV-Young, Older, HIV-Older, and Older*). Boxplot center lines, medians; bounds, interquartile range (IQR); whiskers, 1.5× IQR; dots, individual replicates. Colors as indicated. Two-tailed Student's t-tests with Benjamini–Hochberg FDR correction; adjusted p-values (q): *$p < 0.05$, **$p < 0.01$, ***$p < 0.001$. Comparisons: within-cohort (Control vs LPS) and between-cohort at baseline or after LPS (see panel annotations).



Supplementary Figure 16 | Functional characterization of gene co-expression modules identified by WGCNA module yellow. (a) Network of hub genes in yellow module. (b) Pathway enrichment for the yellow module highlights processes such as neutrophil degranulation, defensins, and antimicrobial peptides, indicating a strong role in innate immune defense. Bubble size corresponds to gene number; color reflects significance ($-\log_{10}$(FDR)). (c) Boxplot of normalized hub gene expression levels across cohorts and conditions of module yellow across five cohorts (Young, HIV-Young, Older, HIV-Older, and Older*). Boxplot center lines, medians; bounds, interquartile range (IQR); whiskers, 1.5× IQR; dots, individual replicates. Colors as indicated. Two-tailed Student's t-tests with Benjamini–Hochberg FDR

correction; adjusted p-values (q): *$p < 0.05$, **$p < 0.01$, ***$p < 0.001$. Comparisons: within-cohort (control vs LPS) and between-cohort at baseline or after LPS (see panel annotations).



Supplementary Figure 17 | Heatmaps and upstream regulator networks across five cohorts. Upstream regulators were filtered by significance (p-value < 0.01) and activation

status (|Z-score| ≥ 2). Regulators meeting these criteria were included in the analysis. An additional expression log ratio (Expr Log Ratio) cutoff of ±3 was applied to highlight regulators with strong expression changes. (a) Activation heatmap: Color intensity reflects positive activation Z-scores (≥ 2), with deeper red indicating stronger activation. Black dots overlay each cell, with dot size proportional to the expression log ratio, representing the magnitude of regulator expression change. (b) Inhibition heatmap: Color intensity reflects negative Z-scores (≤ –2), with deeper blue indicating stronger inhibition. Black dot sizes represent the magnitude of the expression log ratio. (c–f) Upstream regulator networks for IFNB1, TNF, IL1B, and IL6 predicted by IPA, generated using data from the Young cohort only, as network structures were highly similar across cohorts. Each network shows the top 20 predicted downstream targets for the indicated upstream regulator. Node size and edge thickness are proportional to the absolute expression log ratio (|Expr Log Ratio|) of each target gene. Node fill color and border color indicate the predicted activation state: red (upstream regulator), orange (activated target), blue (inhibited target), and grey (affected/other target). Edges are directed from the upstream regulator to each target, with edge color matching the activation state.